Med Chem Res (2013) 22:57–69
DOI 10.1007/s00044-012-0010-5

MEDICINAL CHEMISTRY RESEARCH

ORIGINAL RESEARCH

Molecular drug design, synthesis and pharmacophore site identification of spiroheterocyclic compounds: *Trypanosoma crusi* inhibiting studies

Taibi Ben Hadda · Abdelali Kerbal · Brahim Bennani · Ghali Al Houari · Maria Daoudi · Ana C. L. Leite · Vijay H. Masand · Rahul D. Jawarkar · Zoubida Charrouf

Received: 17 January 2012 / Accepted: 25 February 2012 / Published online: 13 March 2012

Abstract Synthesis and evaluation of the bioactivity of spiroheterocycles (STC) against *Trypanosoma cruzi* are described. Selectivity indices were improved for two compounds versus the leads **17** and **20**, the spiro-thiochromanone (STC) derivatives **17**–**26**, thus increasing the therapeutic interest of our family. As our previous studies conducted on the structure of pharmacophore sites of our compounds made us hypothesize the existence of original sites, STC can be considered as promising tools further anti-trypanosoma studies, as probes for affinity chemotherapy. Compounds **17** and **20** are more potent and more selective than benznidazole and nifurtimox.

T. Ben Hadda (✉)
Laboratoire Chimie Matériaux, Faculté Sciences, Université Mohamed I, Oujda, Morocco
e-mail: taibi.ben.hadda@gmail.com; tbenhadda@yahoo.fr

A. Kerbal · B. Bennani · G. A. Houari · M. Daoudi
Laboratoire Chimie Organique, Université Sidi Mohamed Ben Abdellah, Fès, Morocco

A. C. L. Leite
LabSINFA, DPS-CHS, Federal University of Pernambuco, Recife, Brazil

V. H. Masand
Department of Chemistry, Vidya Bharati College, Camp, Amravati, Maharashtra 444602, India

R. D. Jawarkar
Department of Pharmaceutical Chemistry, Sahyadri College of Pharmacy, Methawade, Sangola, Solapur 413307, Maharashtra, India

Z. Charrouf
Laboratoire Chimie Plantes Synthèse Organique Et Bioorganique, FS, Rabat, Morocco

Keywords *Trypanosoma cruzi* (*TC*) · Spiro-heterocycles · Antiparasitic activity · Drug design · Virtual screening · POM analyzes · Docking studies

Introduction

Benznidazole (Bdz) and nifurtimox (Nfx) have been two of the few most widely used anti-*Trypanosoma cruzi* (*TC*) drugs (Fig. 1). The success of Bdz was mainly due to its outstanding clinical efficacy, and the slow speed at which resistance developed to this drug. But the side effects and the final arrival of resistance and the alarming spread of Bdz-resistant *TC* on a global scale created an urgent need for the development of novel *TC* drugs (Viotti *et al.*, 2009; Pinazo *et al.*, 2010; Moll *et al.*, 2008; Castro and Diaz de Toranzo, 1988; Diaz *et al.*, 2004). So novel anti-trypanosoma drugs were strongly and urgently needed in goal to be used as new drugs without side effects and multi-drug resistance.

Works in our laboratories focus on new spiro-oxazoline-thiochromanones. Our library of spiroheterocycles (STC) derivatives (Badri *et al.*, 1999; Al Houari *et al.*, 2008a, b; Bennani *et al.*, 2002, 2007a, b; Akkurt *et al.*, 2006, 2009; Orhan *et al.*, 2009; Ben Hadda *et al.*, 2008) provided compounds with similar pharmacophore site of clinical drugs Bdz and the Nfx (Fig. 1).

More recently, we have reported a study concerning one series of STC derivatives as antiviral drugs (Orhan *et al.*, 2009). Among them, ten spiro-compounds displayed less toxicity than Bdz and the Nfx, and six of them, compounds **17**–**22** (Fig. 1), have two combined antiviral pharmacophore sites; (O–C–C–O–N) and (S–C–O–N).

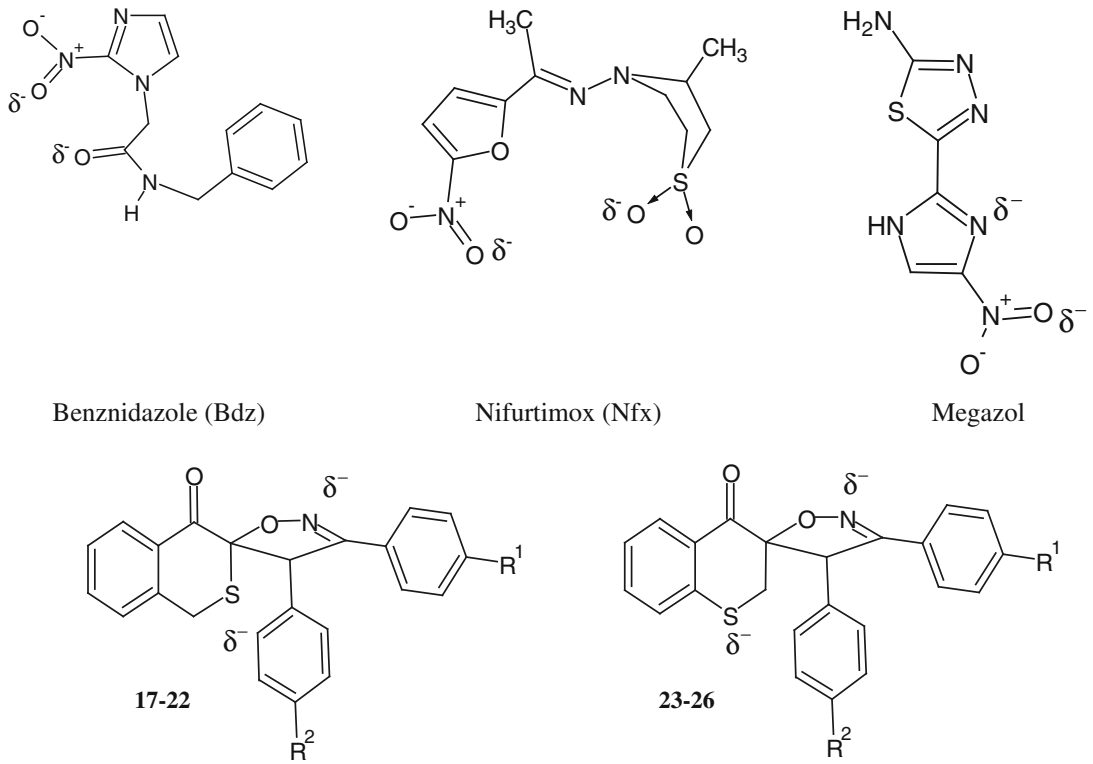

Fig. 1 Structure of candidates spiroheterocyclic compounds **17–26** and clinical antiparasitic agents and their hypothetical S, N and/or O, N-pharmacophore site (Jarrahpour *et al*., 2010)

For all these reasons, compounds **17–22** could represent potential antiparasitic activity for further evaluation as anti-*TC* candidates. Pharmacological studies conducted on compounds suggested a Bdz-like mode of action but also the involvement of additional mechanisms (Anaflous *et al.*, 2004). Bioinformatics studies (Bennani *et al.*, 2007a, b) also suggest the existence of additional combined pharmacophore sites, possibly involving an original mechanism of drug/target interaction.

Considering good pharmacological results obtained in this family, and taking into account some previously established structure-activity relationship, we decided to further enlarge chemical diversity to get more SAR information in our new spiro-oxazole-thiochromanone (SOT) family and in the hope to improve activity/cytotoxicity ratio. First, considering compound Bdz as a reference drug, we decided to introduce chemical diversity at the place of one of the two heterocyclic moieties (Fig. 1). Second, taking into account the important rigidity of spiranic structure in our candidates **17–26**, a high antiparasitic activity is predicted; in our previous series, we decided to replace both flexible pharmacophore sites of reference drugs by more constraint entities; candidates **17–26**.

Chemistry

Synthesis of compounds **19–26**

All synthesized compounds **17–26** were prepared by mixing an equimolar ratio of 3-arylideneisothiochroman-4-ones **11–13** or 3-arylidenethiochroman-4-ones **14–16** and oximes **6–10** in chloroform containing sodium hypochlorite solution (NaOCl, 18°) at 0°C (Scheme 1) which successfully lead to a new series of spiromolecules **22–26**, containing thiochomanone moiety in good yield (81–92%). The reaction was rapid, and no observation supported any kind of side product. All the products were obtained as solids and their purities were checked by thin layer chromatography. All the new synthesized compounds **22–26** were characterized by spectroscopic techniques (IR, ^{1}H NMR, and ^{13}C NMR) and their elemental analyzes. The first series **17–22** is already well known and has been

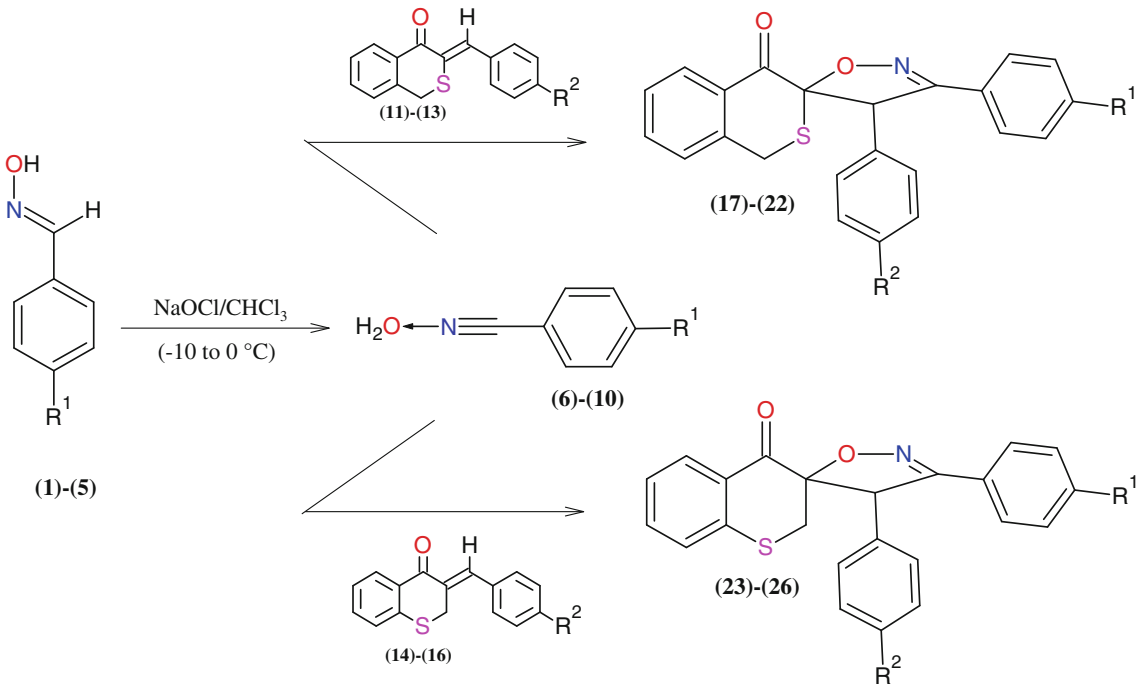

	(R^1)		(R^2)		(R^1, R^2)		(R^1,R^2)
1, 6:	H	**11:**	CH_3	**17:**	(CH_3, CH_3)	**23:**	(H, OCH_3)
2, 7:	CH_3	**12:**	OCH_3	**18:**	(CH_3, OCH_3)	**24:**	(CH_3, H)
3, 8:	OCH_3	**13:**	NO_2	**19:**	(OCH_3, CH_3)	**25:**	(CH_3, OCH_3)
4, 9:	Cl	**14:**	H	**20:**	(OCH_3, OCH_3)	**26:**	(CH_3, NO_2)
5, 10:	NO_2	**15:**	OCH_3	**21:**	(Cl, NO_2)		
		16:	NO_2	**22:**	(NO_2, CH_3)		

Scheme 1 Synthesis of spiroheterocycles **17–26**

previously described by our group (Bennani *et al.*, 2007a, b).

Pharmacology

Biological activity

Antiprotozoan activity (in vitro)

The anti-*TC* activity of the first series of compounds **17–22** is determined by their inhibition of parasite growth using the Bdz-resistant strain. In parallel, all compounds were tested for cytotoxicity upon a BALB/c mice splenocytes. The other new molecules of the series **23–26** were also tested in this same protocol, but none activity was observed at concentration below 100 μg mL^{-1}. Results are given in Table 1.

All compounds **17–26** were tested against *TC* using the Bdz-resistant strain and they were tested for cytotoxicity upon a BALB/c mice splenocytes. The results were compared with those of the standard drugs Bdz and Nfx. All the synthesized compounds exhibited varying degree of inhibitory effect on the growth of different tested strains. A significant activity was observed by all known compounds **17–22** against trypomastigotes and epimastigotes. Compounds **21** and **22** showed moderate activity. Whereas compounds **17**, **19**, and **20** showed significant activity against trypomastigotes. Compounds **17**, **19**, **21**, and **22** showed moderate activity whereas compounds **18** and **20** showed significant activity against epimastigotes. In contrast to new prepared series **23–26**, all the compounds showed moderate to significant activity against *TC* strains. Compound **20** against both trypomastigotes and epimastigotes showed excellent activity. So although most of the compounds showed moderate to significant activity against all parasite strains but compound **20** was the most active one (Table 1).

Results and discussion

Spectroscopic characterizations of **23–26**

In the IR spectra of compounds **23–26**, a characteristic strong band at 1,660–1,684 cm^{-1} is assigned to the

Table 1 *In vitro* bioactivity (IC_{50} in μM) of spiro-heterocyclic compounds **17–26** against *Trypanosoma cruzi*

Compound	R^1	R^2	Cytotoxicity (μg mL^{-1})[a]	IC_{50} (μM)[b] *Trypanosoma cruzi*, Y strain	
				Trypomastigotes at 24 h	Epimastigotes at 11 days
17	CH_3	CH_3	50	3.78	19.1
18	CH_3	OCH_3	5.0	19.0	5.5
19	OCH_3	CH_3	10	1.9	62.5
20	OCH_3	OCH_3	50	1.5	1.95
21	Cl	NO_2	5.0	22.0	20.5
22	NO_2	CH_3	50	45.4	27.9
23	H	OCH_3	Not active	Not active	Not active
24	CH_3	H	Not active	Not active	Not active
25	CH_3	OCH_3	Not active	Not active	Not active
26	CH_3	NO_2	Not active	Not active	Not active
Benznidazole		–	25	5.0	6.6
Nifurtimox		–	1.0 (3.4)	8.5	1.9

[a] Expressed as the highest concentration tested that was not cytotoxic for the BALB/c mice splenocytes. Values in μM are showed in parentheses

[b] Calculated at five concentrations using data obtained from at least three independent experiments, with a SD less than 10% in all cases

Table 2 Selected IR, ^1H and ^{13}C spectral data of series **17–26**

Compd.	Substituents		IR ν (cm^{-1}) ν (CO)	^1H NMR[a]			^{13}C NMR[a]			
	R^1	R^2		H^a	H^b	$H^{4'}$	CH_2	CH	$C^{3'}$	$C^{4'}$
17	CH_3	CH_3	1,675	3.5 $J = 16.8$	4.7	6.10	28.8	56.4	94.6	184.1
18	CH_3	OCH_3	1,675	3.5 $J = 16.8$	4.7	6.1	28.1	57.0	95.0	180.8
19	OCH_3	CH_3	1,675	3.7 $J = 16.8$	4.7	6.1	28.1	56.4	94.4	184.1
20	OCH_3	OCH_3	1,665	3.50 $J = 16.8$	4.7	6.1	28.2	56.2	95.0	184.2
21	CH_3	NO_2	1,680	3.6 $J = 16.8$	4.7	6.2	28.0	56.0	94.4	183.4
22	NO_2	CH_3	1,680	3.6 $J = 16.8$	4.7	6.1	28.1	55.9	95.6	183.6
23	H	OCH_3	1,668	3.0 $J = 14.0$	3.1	5.3	31.9	56.5	86.8	189.2
24	CH_3	H	1,662	3.0 $J = 14.0$	3.0	5.4	31.6	56.7	86.2	188.6
25	CH_3	OCH_3	1,680	3.0 $J = 14.0$	3.1	5.3	31.5	56.2	86.2	188.9
26	CH_3	NO_2	1,684	3.0 $J = 14.0$	3.1	5.4	31.2	56.4	86.7	188.1

[a] ($CDCl_3$, δ ppm/TMS, J in Hz)

stretching of carbonyl C=O group of thio and isothiochromanone moiety. Displacement of this band is an evidence of the formation of condensation product. ^1H NMR spectra of the compounds **17–26** displayed thiomethine (CH_2S) peak at δ 3.0 and 3.1 ppm as doublets for H^a/H^b. H-4′ proton of oxazolyl ring appeared at 5.3–5.5 ppm as singlet. A multiplet was observed at 6.9–7.3 ppm assigned for aromatic protons of phenyl rings. The CH_3 or OCH_3 protons in all cases appeared as a singlet in the region at 2.3 and 3.8 ppm, respectively. Furthermore, the number of the

proton calculated from the integration curves and those obtained from the values of the expected CHN analysis agreed well with each other (Table 2). ^{13}C NMR spectra of compounds **17–26** displayed thiomethine-C (S–$\underline{C}H_2$) peak at 28–32 ppm and an azomethine-C (N=C–$\underline{C}^{4'}$H–) peak at 180–189 ppm which further supported the results obtained in 1H NMR. Compounds **23–26** displayed C^2, C^3/$C^{3'}$, C^4/$C^{4'}$, C^3 ou $C^{5'}$, C^6, C^7 and C^8 carbons of thiochromanone and oxazolyl moiety at 188 ($\underline{C}^4$=O), 86 (spiro-$C^{3,5'}$), 56 ($C^{4'}$), 31 (–S$\underline{C}^2H_2$–), 21 (CH_3), 125, 125, 128, 140, 141, 159, 160 (quaternary aromatic C) and 114; 125, 126, 127, 129, 130, 133 ppm (tertiary aromatic C).

Molecular properties calculations

In series **17–22** the introduction of a variety of fragments by means of the two terminal aryl substituted on positions *para* provided compounds with a broad range of anti-*TC* activities. The highest anti-*TC* activities were obtained for compounds **17** and **20** which exhibited low IC_{50} values between 1.5 and 3.78 μM, up to 5.7-fold lower than Nfx or up to 3.5-fold lower than Bdz.

Replacement of the electron attractor nitro moiety (R^1) in compound **22** by electron donor methyl moiety (R^1) in compounds **17** and **19** provided compounds with activities three to sixfold better than reference drugs (Nfx and Bdz), suggesting that rather bulky and hydrophobic substituents can be introduced in this position without losing activity. Change of sulfur atom's position from S-2 (compounds **17–22** to position S-1) compounds **23–26** of the central ring decrease considerably the anti-*TC* activity when compared to their isomers, compounds **17–22**.

Introduction of R^2 substituent by means of the second aryl link at position C-4′ led to more effective inhibition in the case of derivatives containing electro-donor group as like methoxy or methyl groups. Indeed, activities of the amine compounds **18** and **25**, having the same substituents [(R^1, R^2)=(CH_3, OCH_3)] were found to be completely different; if compound **18** is moderately bioactive (IC_{50} = 19 μM), the later compound **25** and its analogous **23–26** are not active.

Comparison of compounds **17–26** with clinical reference drugs concerning their pharmacophore sites showed that rigidification in this region of our candidates yielded a great win in activity but also a decrease in cytotoxicity, which finally provided for candidates **17–22** important increase in the selectivity index. Further in vivo studies are going to be conducted on compounds **17** and **20** displaying selectivity indices superior to that of reference compounds (Nfx and Bdz). Displacement of the sulfur atom in these compounds **17–26** from position S-2 to S-1 in series of heterocycles **23–26** led to a loss of the ability to inhibit *TC* (with no exception). Inhibition of *TC* strain by our compounds **17–26** appeared thus to be essentially due to the presence of the sulfur atom in position-2, consistent with prediction of hypothetic anti-*TC* pharmacophore site (Fig. 1).

In order to assess the role of lipophilic of terminal aryls and electronic impact on the antiparasitic activity we calculated the partial charges of each heteroatom. Even if our compounds display generally good inhibition of *TC* strain and high intraparasite accumulation by weak-base character, no direct correlation could be established between these parameters and anti-*TC* activity. Exceptions such as aromatic ketone derivatives made us suppose the existence of additional mechanisms. The next step will consist in the search of these putative biological targets by the affinity docking and POM techniques, using the two hits of the series. Compounds **17** or **20** can be considered as good candidates for this technique, as their respective combined pharmacophore sites enable fixation on various targets while preserving significant antiparasitic activities (respective IC_{50} 3.78 and 1.5 μM).

POM virtual screening

Trypanosoma cruzi is much more difficult to treat than human African trypanosoma (HAT), since this trypanosomatid parasite is intracellular, and drugs used for the disease must pass through mammalian and parasite cell membranes to be effective. Laboratory and clinical studies conducted since 1969 have demonstrated that Nfx and Bdz are the best agents for treating human *TC* infection, although they are far from being ideal drugs. Nfx and Bdz are indicated in the acute phase of the infection, the congenital form, reactivation of disease associated with immunosuppression, and in transfusions and organ transplants involving infected individuals. Both drugs are taken orally and must be given divided into 2–3 fractions after meals. They are generally well tolerated by children, particularly in the acute phase of the disease, but relatively frequent and severe gastrointestinal or dermatological adverse reactions may be observed. Recurrence of the disease is a significant problem, and as such these drugs are considered generally ineffective. The main limitations of both drugs are their long courses of administration and the occurrence of adverse side effects. The related compound megazol has also been used for chagas disease, but its use was discontinued because of severe mutagenic and cytotoxic effects (Pinazo *et al*., 2010).

Petra calculations

PETRA is a program package comprising various empirical methods for the calculation of physicochemical

properties in organic molecules. All methods are empirical in nature and have been developed over the last 20 years in the research group of Prof. J. Gasteiger. The following chemical effects can be quantified: heats of formation, bond dissociation energies, sigma charge distribution, *p*-charge distribution, inductive effect, resonance effect and delocalization energies and polarizability effect.

The series **17–26** of STC have been subjected to delocalised-charge calculations using Petra method of the non-hydrogen common atoms, obtained from the partial pi-charge of the heteroatoms, have been used to model the bioactivity against *TC*.

It is found that the negative charges of the sulfur of isothiochromanone moiety and nitrogen atom of oxazol ring contribute positively in favor of antitrypanosomal activity, more, and this is in good agreement with the hypotyhetic mode of antitrypanosomal action of the compounds bearing ($X^{\delta-}/Y^{\delta-}$) pharmacophore site (X, Y=O, N, S), Fig. 1. It was previously hypothesized that difference in charges between two heteroatoms of the same dipolar pharmacophore site ($X^{\delta-}/Y^{\delta+}$) may facilitate the inhibition of bacteria, more than viruses and funguses (Bennani *et al*., 2007a, b); Anaflous *et al.*, 2004; Ben Hadda *et al.*, 2003). It is further found that the activity increases with increase in negative charge of one heteroatom of the common pharmacophore fragment of the hits. The presence of pi-delocalisation phenomena in rigid pharmacophore sites was presented previously since 2007 (*Bennani et al*., 2007a, b).

On the basis of this pharmacophore analog system described above, in compound **17**, sets of distribution of pharmacophore sites in series **17–22** and **23–26** could be considered as probably active in the presence of *TC* and bacteria. This synergistic and streamlined working procedure led to highly active rigid/selective ($X^{\delta-}/Y^{\delta-}$) receptor ligands. However, a little difference in their respective binding affinities was consistently found for the two isomeric series **17–22** and **23–26**. The analysis of isomeric differences due to S heteroatom position (C-1 or C-2) in candidates revealed a favorable ($S^{\delta-}/N^{\delta-}$) interaction in **17–22**, whereas **23–26** showed no activity against *TC*. So the antitrypanosomal activity is related with possible secondary electronic interaction with the positively charged side chains of the virus target(s). Attempt was made to evaluate steric and indicator parameters which emerged as important contributors from previous pharmacologic analysis. The present results support the previous observations that thiochromanone ring in adjacent spiro-position of O–N=C could generate two ($S^{\delta-}/N^{\delta-}$) and ($O^{\delta-}/N^{\delta-}$) pharmacophore sites which are conducive to the activity to anti-HIV ($O^{\delta-}/N^{\delta-}$) (Bennani *et al*., 2007a, b) and antitrypanosomal activity ($S^{\delta-}/N^{\delta-}$).

Osiris calculations

Structure based design is now fairly routine but many potential drugs fail to reach the clinic because of ADME-Tox liabilities. One very important class of enzymes, responsible for many ADMET problems, is the cytochromes P450. Inhibition of these or production of unwanted metabolites can result in many adverse drug reactions. Of the most important program, Osiris is already available online (Rauf *et al.*, 2010; Sheikh *et al.*, 2011; Jawarkar *et al*., 2010a, b, c; Parvez *et al*., 2010a, b, c, d; Chohan *et al.*, 2010a, b, c, d).

The Osiris property explorer shown in this page is an integral part of Actelion's inhouse substance registration system. It lets you draw chemical structures and calculates on-the-fly various drug-relevant properties whenever a structure is valid. Prediction results are valued and color coded. Properties with high risks of undesired effects like mutagenicity or a poor intestinal absorption are shown in red. Whereas a green color indicates drug-conform behavior (Table 3).

With our recent publications of the drug design combination of various pharmacophore sites by using spiro-heterocyclic structure, it is now possible to predict activity and/or inhibition with increasing success in two targets (bacteria and HIV), (Bennani *et al*., 2007a, b). This is done using a combined electronic/structure docking procedure and an example will be given here (Table 3). The remarkably well behaved mutagenicity of divers synthetic molecules classified in data base of CELERON company of Swiss can be used to quantify the role played by various organic groups in promoting or interfering with the way a drug can associate with DNA.

Prediction results are valued and color coded. Properties with high risks of undesired effects like mutagenicity or a poor intestinal absorption are shown in red. Whereas a green color indicates drug-conform behavior (http://www.organic-chemistry.org/prog/peo). *Note*: the side effects most commonly associated with Bdz therapy are rash and gastrointestinal symptoms (nausea). Rarely, peripheral neuropathy may present after prolonged treatment.

Molinspiration calculations

CLogP (octanol/water partition coefficient) is calculated by the methodology developed by molinspiration as a sum of fragment based contributions and correction factors (Table 4). The method is very robust and is able to process practically all organic and most organometallic molecules. Molecular polar surface area TPSA is calculated based on the methodology published by Ertl *et al.* (2000) as a sum of

Table 3 Osiris calculations of compounds **17–22**

Compd.	Toxicity risks				Osiris calculations				
	MUT	TUM	IRRIT	RE	MW	cLog P	Sol	DL	DS
17					399	7.5	−8.1	0.7	0.21
18					415	7.0	−7.8	1.0	0.22
19					415	7.0	−7.8	1.0	0.22
20					431	6.6	−7.5	2.3	0.25
21					450	7.3	−8.6	−6.6	0.12
22					430	7.0	−8.3	−9.2	0.12
Bdz					260	0.6	−1.6	−3.3	0.18
Nfx					301	0.92	−3.4	−2.6	0.47

MUT mutagenic, *TUM* tumorigenic, *IRRIT* irritant, *RE* reproductive effective, *Sol* solubility, *DL* drug-likeness, *DS* drug-score, *Bdz* benznidazole, *Nfx* nifurtimox, the reference drugs

Table 4 Molinspiration calculations of compounds **17–22**

Compd.	(R^1, R^2)	Molinspiration calculations					Drug-likeness			
		cLog P	TPSA	OH/NH	N viol.	Vol.	GPCRL	ICM	KI	NRL
17	(CH_3, CH_3)	6	38	0	1	358	−0.21	−0.37	−0.72	−0.57
18	(CH_3, OCH_3)	5.7	48	0	1	367	−0.20	−0.42	−0.70	−0.54
19	(OCH_3, CH_3)	5.7	48	0	1	367	−0.20	−0.42	−0.70	−0.54
20	(OCH_3, OCH_3)	5.3	57	0	1	376	−0.17	−0.36	−0.66	−0.47
21	(Cl, NO_2)	5.8	85	0	1	362	−0.28	−0.39	−0.77	−0.64
22	(NO_2, CH_3)	5.6	85	0	1	365	−0.32	−0.45	−0.79	−0.63
Bdz	–	0.7	93	1	0	225	−0.39	−0.69	−0.84	−1.55
Nfx	–	1.2	109	0	0	246	−1.24	−1.46	−0.92	−1.49

TPSA total molecular polar surface area, *N viol.* number of violation of five Lipinsky rules, *Vol.* volume, *GPCRL* GPCR ligand, *ICM* ion channel modulator, *KI* kinase inhibitor, *NRL* nuclear receptor ligand

fragment contributions. O– and N– centered polar fragments are considered. PSA has been shown to be a very good descriptor characterizing drug absorption, including intestinal absorption, bioavailability, Caco-2 permeability, and blood–brain barrier penetration. Prediction results of compounds **17–26** molecular properties (TPSA, GPCR ligand and ICM) are valued (Table 4).

Doking of compounds **17–22** in cruzin enzyme

A specific inhibitor of the neuraminidase of the protozoan parasite *TC* was isolated since 1987 and named cruzin (Prioli *et al.*, 1987).

Below is the same diagrams showing interaction of compound **17** with receptor of cruzin. Interestingly, the prominent interactions between the drug and receptor are hydrophobic and arene–arene interactions. No H-bonding is present between drug and receptor (Fig. 2). Figure 2d shows blue—H-bonding donor, red—H-bond acceptor, and white—hydrophobic region. This is receptor based contour map of compound **17**.

From above docking poses, it is clear that during the interaction with cruzin, the six membered ring containing suphur and five membered ring containing N and O are almost perpendicular to each other. From the above analysis it is clear that in ring B, instead of keto group a H-bond donor group like –OH is required (because blue region is very close this group (Fig. 2). In ring D, at *ortho* or *meta* position one hydrophobic group of small size like $–CH_3$ is required (Figs. 2, 3). In ring C, at *ortho* or *meta* or *para* at least one H-bond donor group like –OH or $–NH_2$ is required.

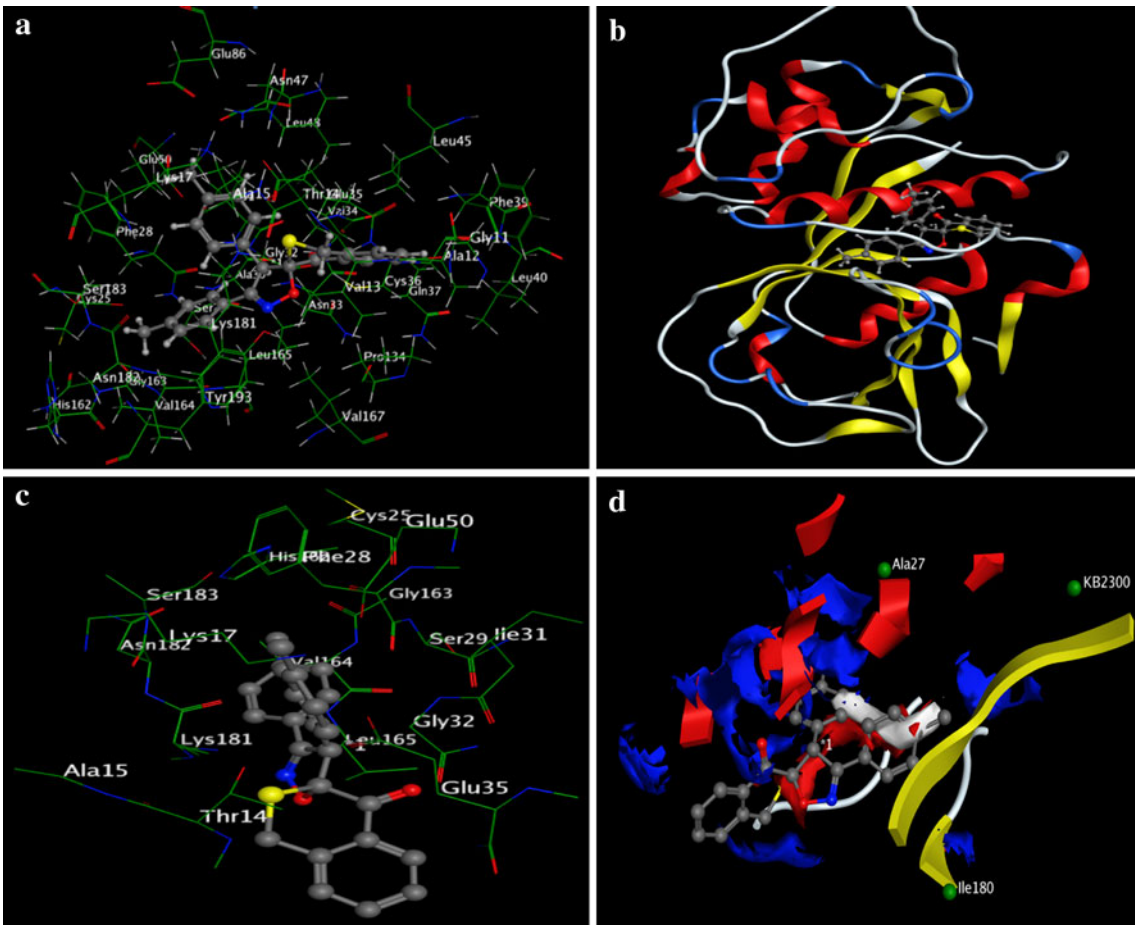

Fig. 2 Docking poses (**a**–**d**) of hit **17** in receptor of cruzin inhibitor

Conclusion

This study provided us with additional structure-activity and structure-cytotoxicity information in the SOT family. Indeed, this study proved that a number of substitutions lead to compounds with high activities and reduced cytotoxicities.

Synthesis and evaluation of the spiroheterocyclic compounds **17–22** showed that lipophilic substituents bearing electro-donor groups could be introduced in oxazolidine moiety while maintaining a high antiparasitic activity. Introduction of sulfur atom in position-1 instead of position-2 on the SOT template provided four additional compounds **23–26** with no anti-parasital activity. Taking into account our first structure-activity relationship, these libraries will include on the terminal aryls of the molecule derivatives of *para*-positions of the two aryl substituents (sugar and hydroxylated groups).

The spiro-molecules bearing ($S^{\delta-}/N^{\delta-}$) pharmacophore site with $d_{S\text{—}N} = 3.5$ A, constitute a potential antitrypanosomal drugs. A similar ($O^{\delta-}/O^{\delta-}$)-pharmacophore is found in curcuminoid analogs with potent activity against *Trypanosoma* and *Leishmania* species (Changtam *et al.*, 2010).

Experimental

Materials and methods

General procedure

^{1}H and ^{13}C NMR spectra were recorded on a Bruker spectrospin spectrometer operating at 80 MHz for ^{1}H (Université Paul Sabatier, Toulouse, France), an AC 200 spectrometer (operating at 200.12 MHz for ^{1}H, 50.32 MHz for ^{13}C), (Université de Franche-Compté, Besançon, France). Chemical shifts are listed in ppm and are reported relative to tetramethylsilane (^{1}H, ^{13}C), residual solvent peaks being used as internal standard. Complete assignments of the ^{13}C spectra required non-decoupled ^{13}C-NMR spectra with selective ^{1}H decoupling. Spectrometers, mass spectra on a Platform II Micro Mass spectrometer, Infrared spectra were obtained on a BECKMAN 310 spectrometer.

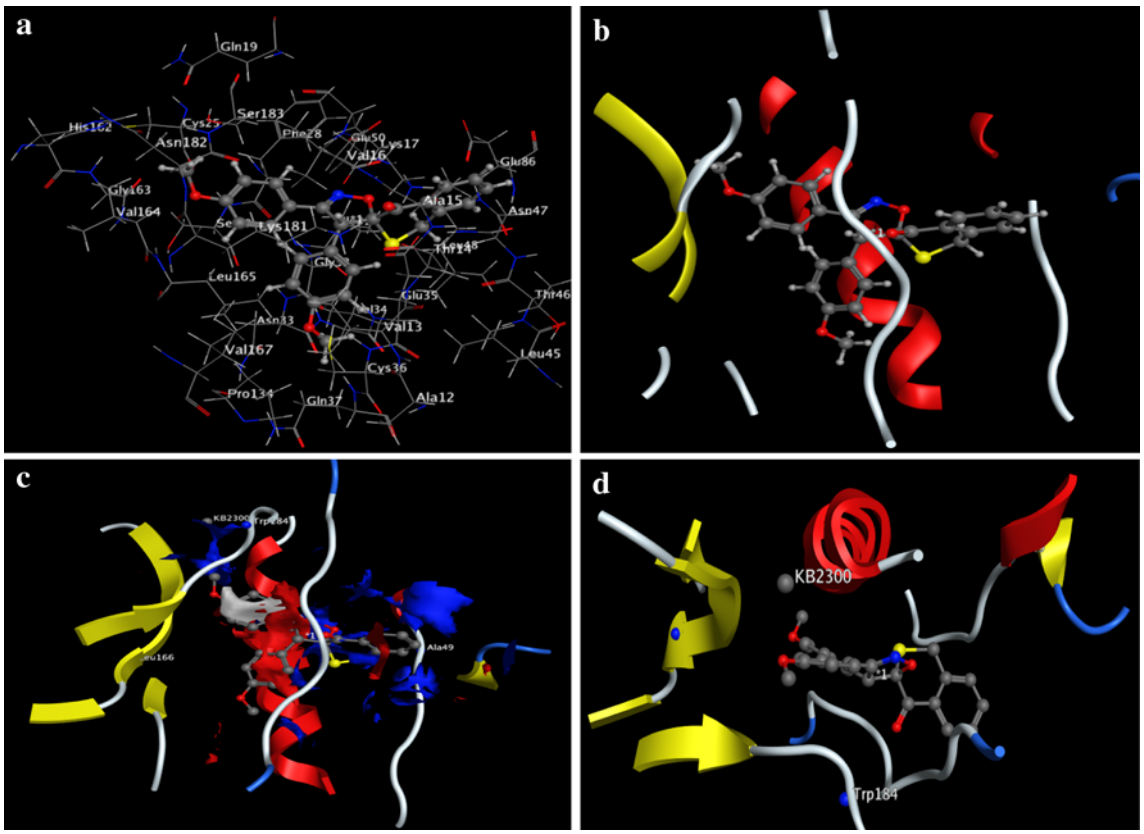

Fig. 3 Docking poses (**a**–**d**) of hit **20** in receptor of cruzin inhibitor

Mass spectra on a HEWLETT PACKARD 5989A Mass spectrometer (70 eV) and elemental analysis (Université Paul Sabatier, Toulouse, France).

*General synthesis of 3′,4′-diaryl-4′H-spiro[isothiochromene-3,5′-isoxazol]-4(1H)-ones **17**–**22** and **23**–**26***

All starting material **1**–**5**, intermediaries **6**–**10** and **11**–**16** have been previously prepared and described by our group in literature (Al Houari *et al.*, 2008a, b; Badri *et al.*, 1999; Ben Hadda *et al.*, 2007, 2008; Bennani *et al.*, 2002, 2007a, b). We report here the synthesis of spiro-molecules **17**–**26**: in an erlenmeyer equipped with a bulb for addition, a mixture of 10 mmol of the 3-arylideneisothiochroman-4-one **11**–**13** or 10 mmol of the 3-arylidenethiochroman-4-one **14**–**16** and 12 mmol of oxime **6**–**10** in 20 ml of chloroform was placed in a ice-salt bath, and under magnetic agitation 10 ml of a sodium hypochlorite solution (NaOCl, 18°) was added. Agitation was maintained for 1 h after the addition. The organic phase was separated, washed several times with water, and dried on sodium sulfate. The residue obtained after evaporation of the solvent was recrystallized from ethanol.

*3′,4′-Di-(4-methyl-phenyl)-4′H-spiro[isothiochromene-3,5′-isoxazol]-4(1H)-one (**17**)*

White powder M.p. = 179°C; yield = 85%, IR (KBr, υ cm^{-1}): 1,675 (C=O). ^{1}H NMR ($CDCl_3$, δ ppm, J Hz): 8.1–7.1 (m, 12H, aromatic H); 6.1 (s, 1H, $CH^{4'}$); 4.7 (d, 1H, H^{1a}, $^{2}JH^{1a}$–H^{1b} = 16.8); 3.50 (d, 1H, H^{1b}, $^{2}JH^{1b}$–H^{1a} = 16.8); 2.5 (s, 3H, CH_3); 2.3 (s, 3H, CH_3). ^{13}C NMR: 184.1 ($\underline{C}^{4}$=O); 94.6 (spiro-$C^{3,5'}$); 56.4 ($C^{4'}$); 28.8 (–S$\underline{C}^{1}H_2$–); 21.5 ($2CH_3$); 125.30; 130.10; 131.40; 138.45; 140.60; 140.85; 160.25 (quaternary aromatic C); 127.50; 127.70; 127.75; 129.30; 129.35; 130.00; 130.45; 132.90 (tertiary aromatic C). Masse spectrum (*m/z*): calc. for $C_{25}H_{21}NSO_2$ (M^+) 399.50; found 399.12. Anal. Calc. for $C_{25}H_{21}NSO_2$: C 75.16; H 5.30; N 3.51; found: C 74.95; H 5.27; N 3.54.

*3′-(4-Methyl-phenyl)-4′-(4-methoxy-phenyl)-4′H-spiro[isothiochromene-3,5′-isoxazol]-4(1H)-one (**18**)*

White powder M.p. = 150°C; yield = 90%. IR (KBr; υ cm^{-1}): 1,675 (C=O). ^{1}H NMR ($CDCl_3$, δ ppm, J Hz): 8.2–6.8 (m, 12H, aromat. H); 6.1 (s, 1H, $CH^{4'}$); 4.7 (d, 1H, H^{1a}, $^{2}JH^{1a}$–H^{1b} = 16.8); 3.7 (s, 3H, OCH_3); 3.5 (d, 1H, H^{1b}, $^{2}JH^{1b}$–H^{1a} = 16.8); 2.3 (s, 3H, CH_3). ^{13}C NMR: 180.8

($\underline{C}^4$=O); 95.0 (spiro-$C^{3,5'}$); 57.0 ($C^{4'}$); 55.0 (OCH_3); 28.1 (–S$\underline{C}^1H_2$–); 21.1 (CH_3); 120.50; 130.15; 131.35; 138.40; 140.90; 159.80; 161.20 (quaternary aromatic C); 114.10; 127.50; 127.80; 129.30; 129.35; 130.10; 131.40; 132.90 (tertiary aromatic C). Masse spectrum (*m/z*): calc. for $C_{25}H_{21}NSO_3$ (M^+) 415.50; found 415.12. Anal. Calc. for $C_{25}H_{21}NSO_3$: C 72.27; H 5.09; N 3.37; found: C 70.08; H 4.97; N 3.41.

*3′-(4-Methoxy-phenyl)-4′-(4-methyl-phenyl)-4′H-spiro[isothiochromene-3,5′-isoxazol]-4(1H)-one (**19**)*

White powder M.p. = 153–155°C; yield = 90%; IR (KBr, υ cm^{-1}): 1,675 (C=O). ^1H NMR ($CDCl_3$, δ ppm, J Hz): 8.1–6.7 (m, 12H, aromatic H); 6.1 (s, 1H, $CH^{4'}$); 4.7 (d, 1H, H^{1a}, $^2JH^{1a}$–H^{1b} = 16.8); 3.70 (s, 3H, OCH_3); 3.5 (d, 1H, H^{1b}, $^2JH^{1b}$–H^{1a} = 16.8); 2.3 (s, 3H, CH_3). ^{13}C NMR: 184.1 ($\underline{C}^4$=O); 94.4 (spiro-$C^{3,5'}$); 56.4 ($C^{4'}$); 55.2 (OCH_3); 28.1 (–S$\underline{C}^1H_2$–); 21.3 (CH_3); 120.50; 130.20; 131.35; 138.45; 140.90; 159.85; 161.20 (quaternary aromatic C); 114.10; 127.55; 127.80; 129.35; 130.05; 130.40; 132.95 (tertiary aromatic C). Masse spectrum (*m/z*): calc. for $C_{25}H_{21}NSO_3$ (M^+) 415.50; found 415.12. Anal. Calc. for $C_{25}H_{21}NSO_2$: C 72.27; H 5.09; N 3.37; found: C 71.98; H 4.97; N 3.41.

*3′,4′-Di-(4-methoxy-phenyl)-4′H-spiro[isothiochromene-3,5′-isoxazol]-4(1H)-one (**20**)*

White powder M.p. = 154–156°C; yield = 85%; IR (KBr; υ cm^{-1}): 1,665 (C=O). ^1H NMR ($CDCl_3$, δ ppm, J Hz): 8.1–6 (m, 12H, aromat. H); 6.1 (s, 1H, $CH^{4'}$); 4.7 (d, 1H, H^{1a}, $^2JH^{1a}$–H^{1b} = 16.8); 3.7 (s, 6H, 2 OCH_3); 3.5 (d, 1H, H^{1b}, $^2JH^{1b}$–H^{1a} = 16.8). ^{13}C NMR: 184.2 ($\underline{C}^4$=O); 95.0 (spiro-$C^{3,5'}$); 56.2 ($C^{4'}$); 55.3 (2OCH_3); 28.2 (–S$\underline{C}^1H_2$–); 120.50; 125.15; 130.40; 131.40; 140.90; 159.70; 159.80; 161.20 (quaternary aromatic C); tertiary aromatic C: 113.90; 114.10; 127.50; 127.75; 129.35; 130.40; 131.30; 132.90 (tertiary aromatic C). Masse spectrum (*m/z*): calc. for $C_{25}H_{21}NSO_4$ (M^+) 431.50; found 431.11. Anal. Calc. for $C_{25}H_{21}NSO_4$: C 69.59; H 4.91; N 3.25; found: C 69.83; H 5.13; N 3.15.

*3′-(4-Chloro-phenyl)-4′-(4-nitro-phenyl)-4′H-spiro[isothiochromene-3,5′-isoxazol]-4(1H)-one (**21**)*

White powder M.p. = 149–151°C; yield = 60%; IR (KBr; υ cm^{-1}): 1,665 (C=O). ^1H NMR ($CDCl_3$, δ ppm, J Hz): 8.2–7.2 (m, 12H, aromat. H); 6.2 (s, 1H, CH^4); 4.7 (d, 1H, H^{1a}, $^2JH^{1a}$–H^{1b} = 16.8); 3.6 (d, 1H, H^{1b}, $^2JH^{1b}$–H^{1a} = 16.8); ^{13}C NMR: 183.4 ($\underline{C}^4$=O); 94.4 ($C^{3,5'}$); 56.0 ($C^{4'}$); 28.0 (–S$\underline{C}^1H_2$–); 125.90; 130.75; 137.60; 139.80; 140.40; 148.10; 158.55 (qquaternary aromatic C); 123.80; 127.80; 127.90; 128.80; 129.25; 130.50; 131.10; 133.40 (tertiary aromatic C). Masse spectrum (*m/z*): calc. for $C_{23}H_{15}N_2O_4ClS$ (M^+) 450.89; found 450.05. Anal. Calc. for $C_{23}H_{15}N_2O_4ClS$: C 61.27; H 3.35; N 6.21; found: C 60.95; H 3.26; N 6.28.

*3′-(4-Nitro-phenyl)-4′-(4-methyl-phenyl)-4′H-spiro[isothiochromene-3,5′-isoxazol]-4(1H)-one (**22**)*

White powder M.p. = 187–189°C; yield = 65%; IR (KBr; υ cm^{-1}): 1,680 (C=O). ^1H NMR ($CDCl_3$, δ ppm, J Hz): 8.1–7.1 (m, 12H, aromatic H); 6.1 (s, 1H, $CH^{4'}$); 4.7 (d, 1H, H^{1a}, $^2JH^{1a}$–H^{1b} = 16.8); 3.6 (d, 1H, H^{1b}, $^2JH^{1b}$–H^{1a} = 16.8); 2.3 (s, 3H). ^{13}C NMR: 183.6 ($\underline{C}^4$=O); 95.6 (spiro-$C^{3,5'}$); 55.9 ($C^{4'}$); 28.1 (–S$\underline{C}^1H_2$–); 21.3 (CH_3); 128.50; 130.00; 131.00; 139.15; 140.70; 148.60; 158.80 (quaternary aromatic C); 123.90; 127.75; 127.90; 128.10; 128.80; 129.05; 129.65; 130.90 (tertiary aromatic C). Masse spectrum (*m/z*): calc. for $C_{24}H_{18}N_2SO_4$ (M^+) 430.47; found 430.09. Anal. Calc. for $C_{24}H_{18}N_2SO_4$: C 66.96; H 4.21; N 6.51; found: C 67.12; H 4.18; N 5.95.

*3′-Phenyl-4′-(4-methoxy-phenyl)-4′H-spiro[thiochromene-3,5′-isoxazol]-4(1H)-one (**23**)*

White powder M.p. = 183–185°C; yield = 87%. IR (KBr; υ cm^{-1}): 1,668 (C=O). ^1H NMR ($CDCl_3$, δ ppm, J Hz): 8.13–6.9 (m, 13H, aromat. H); 5.36 (s, 1H, $CH^{4'}$); 3.8 (s, 3H, OCH_3); 3.14 (d, 1H, H^{2b}, $^2JH^{2a}$–H^{2b} = 14.01); 3.05 (d, 1H, H^{2a}, $^2JH^{2a}$–H^{2b} = 14.01). ^{13}C NMR: 189.3 ($\underline{C}^4$=O); 86.81 (spiro-$C^{3,5'}$); 56.5 ($C^{4'}$); 55.67 (OCH_3); 31.91 (–S$\underline{C}^2H_2$–); 128.73; 129.23; 130.60; 130.60; 141.75; 160.09; 160.56 (quaternary aromatic C); 115.03; 125.39; 125.47; 127.04; 127.95; 128.98; 131.37; 134.19 (tertiary aromatic C). Masse spectrum (*m/z*): calc. for $C_{24}H_{19}NO_3S$ (M^+) 401.47; found 401.11. Anal. Calc. for $C_{24}H_{19}NO_3S$: C 71.91; H 4.73; N 6.51; found: C 67.12; H 4.18; N 53; found: C 71.80; H 4.77; N 3.49.

*3′-(4-Methyl-phenyl)-4′-phenyl-4′H-spiro[thiochromene-3,5′-isoxazol]-4(1H)-one (**24**)*

White powder M.p. = 192–193°C; yield = 92%; IR (KBr; υ cm^{-1}): 1,662 (C=O). ^1H NMR ($CDCl_3$, δ ppm, J Hz): 8.13–6.9 (m, 13H, aromat. H); 5.4 (s, 1H, $CH^{4'}$); 3.14 (d, 1H, H^{2b}, $^2JH^{2a}$–H^{2b} = 14.01); 3.05 (d, 1H, H^{2a}, $^2JH^{2a}$–H^{2b} = 14.01); 2.3 (s, 3H, CH_3). ^{13}C NMR: 186.2 ($\underline{C}^4$=O); 86.2 (spiro-$C^{3,5'}$); 56.7 ($C^{4'}$); 31.6 (–S$\underline{C}^2H_2$–); 21.5 (CH_3); 125.37; 128.82; 133.42; 140.55; 141.35; 160.12 (quaternary aromatic C); 125.07; 126.64; 127.51; 128.53; 129.26; 129.34; 130.99 (tertiary aromatic C). Masse spectrum (*m/z*): calc. for $C_{24}H_{19}NO_2S$ (M^+) 385.47; found 385.11. Anal. Calc. for $C_{24}H_{19}NO_2S$: C 74.78; H 4.97; N 3.63; found: C 74.37; H 4.85; N 3.49.

*3′-(4-Methyl-phenyl)-4′-(4-methoxy-phenyl)-4′H-spiro[thiochromene-3,5′-isoxazol]-4(1H)-one (**25**)*

White powder M.p. = 172–174°; yield = 85%; IR (KBr; υ cm^{-1}): 1,680 (C=O). ^1H NMR ($CDCl_3$, δ ppm, J Hz): 8.1–6.9 (m, 12H, aromat. H); 5.4 (s, 1H, $CH^{4'}$); 3.8 (s, 3H, OCH_3); 3.13 (d, 1H, H^{2b}, $^2JH^{2a}$–H^{2b} = 14.01); 3.04 (d, 1H, H^{2a}, $^2JH^{2a}$–H^{2b} = 14.01); 2.3 (s, 3H, CH_3). ^{13}C NMR: 188.96 ($\underline{C}^4$=O); 86.2 (spiro-$C^{3,5'}$); 56.24 ($C^{4'}$); 31.51 (–S$\underline{C}^2H_2$–); 21.45 (CH_3); 125.13; 125.43; 128.84; 140.48; 141.33; 159.68; 160.10 (quaternary aromatic C); 114.56; 125.05; 126.63; 127.49; 129.30; 130.96; 133.73 (tertiary aromatic C). Masse spectrum (*m*/*z*): calc. for $C_{25}H_{21}NO_3S$ (M^+) 415.50; found 415.12. Anal. Calc. for $C_{25}H_{21}NO_3S$: C 72.27; H 5.09; N 3.37; found: C 71.98; H 4.98; N 3.41.

*3′-(4-Methyl-phenyl)-4′-(4-nitro-phenyl)-4′H-spiro[thiochromene-3,5′-isoxazol]-4(1H)-one (**26**)*

White powder M.p. = 194–196°C; yield = 81%; IR (KBr; υ cm^{-1}): 1,684 (C=O). ^1H NMR ($CDCl_3$, δ ppm, J Hz): 8.3–7.1 (m, 12H, aromat. H); 5.46 (s, 1H, $CH^{4'}$); 3.12 (d, 1H, H^{2b}, $^2JH^{2a}$–H^{2b} = 14.01); 3.03 (d, 1H, H^{2a}, $^2JH^{2a}$–H^{2b} = 14.01); 2.31 (s, 3H, CH_3). ^{13}C NMR: 188.15 ($\underline{C}^4$=O); 86.77 (spiro-$C^{3,5'}$); 56.46 ($C^{4'}$); 31.24 (–S$\underline{C}^2H_2$–); 21.45 (CH_3); 124.58; 129.57; 134.48; 140.87; 147.97; 141.61; 159.36 (quaternary aromatic C); 124.37; 125.39; 126.72; 127.38; 129.57; 130.20; 131.14; 134.11 (tertiary aromatic C). Masse spectrum (*m*/*z*): calc. for $C_{24}H_{18}N_2O_4S$ (M^+) 430.47; found 430.09. Anal. Calc. for $C_{24}H_{18}N_2O_4S$: C 66.96; H 4.21; N 6.51; found: C 67.02; H 4.17; N 6.48.

Biological properties

Antitypanosomal activity (in vitro)

The anti-*TC* activities of the compounds were determined by their inhibition of parasite growth using the Bdz-resistant strain. In parallel, all compounds were tested for cytotoxicity upon a BALB/c mice splenocytes. All compounds were tested against *TC* using the Bdz-resistant strain and they were tested for cytotoxicity upon a BALB/c mice splenocytes.

In vitro cytotoxicity

The cytotoxicity of compounds was determined using BALB/c mice splenocytes (5×10^6 cells $well^{-1}$) cultured in 96-well plates in Dulbecco's modified eagle's medium (DMEM, Sigma Chemical Co., St. Louis, MO) supplemented with 10% of fetal calf serum (FCS; Cultilab, Campinas, SP, Brazil) and 50 μg mL^{-1} of gentamycin (Novafarma, Anápolis, GO, Brazil). Each compound was evaluated at five concentrations (1, 2, 5, 10, 25, 50, and 100 μg mL^{-1}), in triplicate. Cultures were incubated in the presence of ^3H-thymidine (1 μCi $well^{-1}$) for 24 h at 37°C and 5% CO_2. After this period, the content of the plate was harvested to determine ^3H-thymidine incorporation using a beta-radiation counter (LKB Wallac Rack Beta, Pharmacia Biotech). The cytotoxicity of the compounds was determined by comparing the percentage of ^3H-thymidine incorporation (as an indicator of cell viability) in drug-treated wells in comparison to untreated wells. Non-cytotoxic concentrations were defined as those causing a reduction of ^3H-thymidine incorporation below 10% in relation to untreated controls.

In vitro antiproliferative activity

Epimastigotes of *TC* (Y strain) were cultivated at 26°C in liver infusion tryptose medium (LIT) supplemented with 10% fetal calf serum, 1% hemin, 1% R9 medium, and 50 μg mL^{-1} gentamycin. Parasites (10^6 cells mL^{-1}) were cultured in a fresh medium in the absence or in the presence of the compounds being tested (from stock solution in DMSO). Cell growth was determined after 11 days of culture by counting viable forms in a hemacytometer, in triplicate. The spiro-heterocycles compounds used were from a stock solution in DMSO. To determine the IC_{50}, cultures of Y strain epimastigotes in the presence of different concentrations of the compounds were evaluated after 11 days as described above. IC_{50} calculation was carried out using non-linear regression on Prism 4.0 GraphPad software. Biological assays on Y strain *TC* trypomastigotes were obtained from culture supernatants of vero cell line at 37°C and placed in 96-well plates (4×10^5 $well^{-1}$) in a DMEM medium supplemented with 10% FCS and 50 μg mL^{-1} gentamycin. Viable parasites were counted in a hemacytometer 24 h after addition of complexes by way of trypan blue exclusion. The percentage of inhibition was calculated in relation to untreated cultures. The same procedure was performed for Bdz and Nfx (reference drugs) and vehicle alone, DMSO as blank.

Acknowledgments We are grateful to staff of Federal University of Pernambuco, Recife-Brazil for the help in biological assay. Prof. T. Ben Hadda would like to thank the ACTELION; the Biopharmaceutical Company of Swiss, for the online molecular properties calculations.

References

Akkurt M, Yildirim SO, Badri R, Kerbal A, Ben Hadda T, Buyukgungor O (2006) 4-*p*-Anisyl-1,2′-diphenyl-3-*p*-tolyl-2′,3′-dihydro-spiro[2-pyrazoline-5,3,0-isoquinolin]-4′(1′*H*)-one. Acta Cryst E62:o5022–o5023

Akkurt M, Yıldırım SÖ, Kerbal A, Bennani B, Daoudi M, Chohan ZH, McKee V, Ben Hadda T (2009) Crystal structure of 3′-(4-methoxyphenyl)-2-phenyl-4′-(4-ethoxyphenyl)-1,2-dihydro-4*H*,4′*H*-spiro [isoquinoline-3,5′-isoxazol]-4-one. J Chem Crystallogr. doi:10.1007/s10870-009-9639-4

Al Houari G, Kerbal A, Larbi NB, Bennani B, Ben Hadda T, Stoeckli-Evans H (2008a) 4′-Methyl-3-(4-nitrophenyl)-4-phenyl-4,5,1′,2′,3′,4′-hexahydrospiro[isoxazole-5,2′-naphthalen]-1′-one. Acta Cryst E64:o509–o510

Al Houari G, Kerbal A, Bennani B, Baba MF, Daoudi M, Ben Hadda T (2008b) Drug design of new antitubercular agents: 1,3-dipolar cycloaddition reaction of arylnitriloxides and 3-*para*-methoxybenzylidene-isochroman-4-ones. Arkivoc xii:42–50

Anaflous A, Benchat N, Mimouni M, Abouricha S, Ben Hadda T, El-Bali B, Hakkou A, Hacht B (2004) Armed imidazo [1,2-*a*] pyrimidines (pyridines):evaluation of antibacterial activity. Lett Drug Des Discov 1:224–229

Badri R, Kerbal A, Najib B, El-Bali B, Escudie J, Ranaivonjatovo H, Bolte M (1999) 3′-(*p*-Nitrophenyl)-2-phenyl-4′-(*p*-tolyl)spiro [isoquinoline-3(2*H*),5′(4′*H*)-isoxazolin]-4(1*H*)-one. Acta Cryst C55. IUC9900165

Ben Hadda T, Benchat N, El-Bali B, Abouricha S, Moueqqit M, Mimouni M. (2003) Impact of dimroth rearrangement on antituberculosis activity of 3-armed-imidazo[1,2-*a*]pyrimidines IMP (-pyridines) IP. Med Pharm Chem 1–18 online. Paper N°: 0301001

Ben Hadda T, Badri R, Kerbal A, Filali Baba B, Akkurt M, Demailly G, Benazza M (2007) Synthesis and antitubercular activity of spiroheterocycles: 2,2′,4′,5′-tetra-substituted-1,2,2′,4′-tetrahydro-4*H*-spiro[isoquinoline-3,3′-pyrazol]-4-ones. Arkivoc xiv: 276–288

Ben Hadda T, Badri R, Kerbal A, Bennani B, Al Houari G, Filali Baba B, Akkurt M, Demailly G, Benazza M (2008) Looking for a new antitubercular pharmacophore site: synthesis and bioactivity of spiroheterocycles 2,3′,4′-tri-subsituted-1,2-dihydro-4*H*,4′*H*-spiro [isoquinoline-3,5′-isoxazol]-4-ones. Arkivoc ii:1–13

Bennani B, Filalibaba B, El-Fazazi A, Houari GA, Bitit N, Kerbal A, El-Bali B, Bolte M (2002) 2′,3′-Diphenyl-4′-*p*-tolylspiro[isothiachroman-3,5′-isoxazolidin]-4(2*H*)-one. Acta Cryst E58:o312–o313

Bennani B, Jalbout AF, Baba BF, Larbi NB, Boukir A, Kerbal A, Mimouni M, Ben Hadda T, Trzaskowski B (2007a) Synthesis of new spiro-[isothiochromene-3,5′-isoxazolidin]-4(1*H*)-ones. Heterocycl Chem 44(3):711–716

Bennani B, Kerbal A, Daoudi M, Filali Baba B, Al Houari G, Jalbout AF, Mimouni M, Benazza M, Demailly G, Akkurt M, Yýldýrým SÖ, Ben Hadda T (2007b) Combined drug design of potential *Mycobacterium tuberculosis* and HIV-1 inhibitors: 3′,4′-disubstituted-4′*H*-spiro[isothiochromene-3,5′-isoxazol]-4(1*H*)-one. Arkivoc xvi:19–40

Castro JA, Diaz de Toranzo EG (1988) Toxic effects of nifurtimox and benznidazole, two drugs used against American trypanosomiasis (Chagas' disease). Biomed Environ Sci 1(1):19–33

Changtam C, de Koning HP, Ibrahim H, Sajid MS, Gould MK, Suksamrarn A (2010) Curcuminoid analogs with potent activity against *Trypanosoma* and *Leishmania* species. Eur J Med Chem 45:941–956

Chohan ZH, Sumrra SH, Youssoufi MH, Ben Hadda T (2010a) Metal based biologically active compounds: design, synthesis and antibacterial/antifungal/cytotoxic properties of triazole derived Schiff bases and their oxovanadium(IV) complexes. Eur J Med Chem 45:2739–2747

Chohan ZH, Youssoufi MH, Jarrahpour A, Ben Hadda T (2010b) Identification of antibacterial and antifungal pharmacophore sites for potent bacteria and fungi inhibition: indolenyl sulfonamide derivatives. Eur J Med Chem 45:1189–1199

Chohan ZH, Sumrra SH, Youssoufi MH, Ben Hadda T (2010c) Design and synthesis of triazole schiff bases and their oxovanadium(IV) complexes as antimicrobial agents. J Coord Chem 63(22):3981–3998

Chohan ZH, Shad HA, Toupet L, Ben Hadda T, Akkurt M (2010d) Structure of a new bioactive agent containing combined antibacterial and antifungal pharmacophore sites: 4-{[(E)-(5-bromo-2-hydroxyphenyl)methylidene]amino}-*N*-(5-methyl-1,2-oxazol-3-yl)benzene-sulfonamide. J Chem Crystallogr. doi: 10.1007/s10870-010-9856-x

Diaz EG, Montalto DMM, Castro JA (2004) Reactions of nifurtimox with critical sulfhydryl-containing biomolecules: their potential toxicological relevance. J Appl Toxicol 24(3):189–195

Ertl P, Rohde B, Selzer P (2000) Fast calculation of molecular polar surface area as a sum of fragment-based contributions and its application to the prediction of drug transport properties. J Med Chem 43(20):3714–3717

Jarrahpour A, Motamedifar M, Zareil M, Youssoufi MH, Mimouni M, Chohan ZH, Ben Hadda T (2010) Petra, osiris and molinspiration together as a guide in drug design: predictions and correlation structure/antibacterial activity relationships of new *N*-sulfonyl monocyclic β-lactams (part II). Phosphorus, Sulfur, Silicon Relat Elem 185:491–497

Jawarkar RD, Mahajan DT, Masand VH, Ben Hadda T, Kurhade GH (2010a) COMFA analysis and toxicity risk assessment of coumarin analogues as Mao-A inhibitors: attempting better insight in drug design. Der Pharm Lett 2(6):350–357

Jawarkar RD, Masand VH, Patil KN, Mahajan DT, Youssoufi MH, Ben Hadda T, Kumbhare SL (2010b) 3D-QSAR study on coumarin analogues as potent inhibitors of MAO-B using a CoMFA approach. Der Pharm Chem 2(6):302–310

Moll C, Peris C, Moreno A, Muñoz J, Guañabens N (2008) Severe invalidating pain syndrome associated with benznidazole therapy for Chagas' disease. Clin Rheumatol 27(2):269–270

Orhan İ, Şenol FS, Khan MTH, Ben Hadda T, Bennani B, Kerbal A, Şener B (2009) Acetylcholinesterase inhibitory potentials of several synthetic spiro-heterocycles. International symposium on pharmaceutical sciences, Ankara, 23–26 June

Parvez A, Jyotsna M, Sheikh J, Tiwari V, Dongre R, Ben Hadda T (2010) Predictions and correlations of structure activity relationship of some aminoantipyrine derivatives on the basis of theoretical and experimental ground. Med Chem Res. doi: 10.1007/s00044-010-9505-0

Parvez A, Meshram J, Tiwari V, Sheikh J, Dongre R, Shanti M, Khandarkar K, Ahemad M, Ben Hadda T (2010b) Greener synthetic and nanotechnological bridge: theoretical and practical biological approach toward the bactericidal dual action mechanism of azomethine–nanosilver hybrid. Int J Green Nanotech: Phys Chem 2(2):53–61

Parvez A, Meshram J, Youssoufi MH, Ben Hadda T (2010c) Theoretical calculations and experimental verification of the antibacterial potential of some monocyclic beta-lactames containing two synergetic buried antibacterial pharmacophore sites. Phosphorus, Sulfur Silicon Relat Elem 7:1500–1510

Parvez A, Meshram J, Tiwari V, Sheikh J, Dongre R, Youssoufi MH, Ben Hadda T (2010d) Pharmacophores modeling in terms of prediction of theoretical physicochemical properties and verification by experimental correlations of novel coumarin derivatives produced via Betti's protocol. Eur J Med Chem 45(9): 4370–4378

Pinazo M-J, Muñoz J, Posada E, López-Chejade P, Gállego M, Ayala E, Del Cacho E, Soy D, Gascon J (2010) Tolerance of benznidazole in treatment of Chagas' disease in adults. Antimicrob Agents Chemother 54(11):4896–4899

Prioli RP, Ordovas JM, Rosenberg I, Schaefer EJ, Pereira ME (1987) Similarity of cruzin, an inhibitor of *Trypanosoma cruzi*

neuraminidase, to high-density lipoprotein. Science 238(4832): 1417–1419

Rauf A, Liaqat S, Qureshi AM, Yaqub M, Rehman AU, Hassan MU, Chohan ZH, Nasim Faiz UH, Ben Hadda T (2010) Synthesis, characterization, and urease inhibition of 5-substituted-8-methyl-2*H*-pyrido[1,2-*a*]pyrimidine-2,4(3*H*)-diones. Med Chem Res. doi:10.1007/s00044-010-9491-2

Sheikh J, Parvez A, Ingle V, Juneja H, Dongre R, Chohan ZH, Youssoufi MH, Ben Hadda T (2011) Synthesis, biopharmaceutical characterization, antimicrobial and antioxidant activities of 1-(4′-O-β-D-glucopyranosyloxy-2′-hydroxyphenyl)-3-aryl-propane-1,3-diones. Eur J Med Chem 46: 1390–1399

Viotti R, Vigliano C, Lococo B, Alvarez MG, Petti M, Bertocchi G, Armenti A (2009) Tolerance of benznidazole in treatment of Chagas' disease in adults. Exp Rev Anti Infect Ther 7(2): 157–163